

Short communication

Monitoring vegetation phenology using MODIS

Xiaoyang Zhang^{a,*}, Mark A. Friedl^a, Crystal B. Schaaf^a, Alan H. Strahler^a,
John C.F. Hodges^a, Feng Gao^a, Bradley C. Reed^b, Alfredo Huete^c^aDepartment of Geography and Center for Remote Sensing, Boston University, 675 Commonwealth Avenue, Boston, MA 02215, USA^bEROS Data Center, Sioux Falls, SD 57198, USA^cDepartment of Soil and Water Science, University of Arizona, Tucson, AZ 85721, USA

Received 25 May 2002; received in revised form 6 September 2002; accepted 7 September 2002

Abstract

Accurate measurements of regional to global scale vegetation dynamics (phenology) are required to improve models and understanding of inter-annual variability in terrestrial ecosystem carbon exchange and climate–biosphere interactions. Since the mid-1980s, satellite data have been used to study these processes. In this paper, a new methodology to monitor global vegetation phenology from time series of satellite data is presented. The method uses series of piecewise logistic functions, which are fit to remotely sensed vegetation index (VI) data, to represent intra-annual vegetation dynamics. Using this approach, transition dates for vegetation activity within annual time series of VI data can be determined from satellite data. The method allows vegetation dynamics to be monitored at large scales in a fashion that it is ecologically meaningful and does not require pre-smoothing of data or the use of user-defined thresholds. Preliminary results based on an annual time series of Moderate Resolution Imaging Spectroradiometer (MODIS) data for the northeastern United States demonstrate that the method is able to monitor vegetation phenology with good success.

© 2002 Elsevier Science Inc. All rights reserved.

Keywords: Vegetation phenology; MODIS; Remote sensing

1. Introduction

The phenological dynamics of terrestrial ecosystems reflect response of the Earth's biosphere to inter- and intra-annual dynamics of the Earth's climate and hydrologic regimes (Myneni, Keeling, Tucker, Asrar, & Nemani, 1997; Schwartz, 1999; White, Thornton, & Runnings, 1997). Because of the synoptic coverage and repeated temporal sampling that satellite observations afford, remotely sensed data possess significant potential for monitoring vegetation dynamics at regional to global scales (e.g., Myneni et al., 1997). In the last decade, a number of different methods have been developed to determine the timing of vegetation greenup and senescence (i.e., the start and end of growing season) using time series of normalized difference vegetation index (NDVI) data from the Advanced Very High Resolution Radiometer (AVHRR). These methods have employed a variety of different approaches including the use of specific

NDVI thresholds (Lloyd, 1990; White et al., 1997), the largest NDVI increase (Kaduk & Heimann, 1996), backward-looking moving averages (Reed et al., 1994), or empirical equations (Moulin, Kergoat, Viovy, & Dedieu, 1997). However, such methods are difficult to apply at global scales, and generally do not account for ecosystems characterized by multiple growth cycles (e.g., double- or triple-crop agriculture, semiarid systems with multiple rainy seasons, etc.).

Satellite vegetation index (VI) data such as the NDVI are correlated with green leaf area index (LAI), green biomass, and percent green vegetation cover (Asrar, Myneni, & Kanemasu, 1989; Baret & Guyot, 1991). Until recently, the AVHRR provided the only source of global data for this purpose. However, because the AVHRR was never designed for land applications, these data are not well suited for vegetation monitoring applications. Specifically, the lack of precise calibration, poor geometric registration, and difficulties involved in cloud screening AVHRR data result in high levels of noise (Goward, Markham, Dye, Dulaney, & Yang, 1991). The radiometric and geometric properties of the Moderate Resolution Imaging Spectroradiometer (MODIS) onboard NASA's Terra spacecraft, in combination

* Corresponding author.

E-mail address: zhang@crsa.bu.edu (X. Zhang).

with improved atmospheric correction and cloud screening provided by MODIS science team activities, provide a substantially improved basis for studies of this nature. In this paper, we present the first attempt to study vegetation phenology using data from MODIS.

2. Monitoring phenology using remote sensing

For this work, the annual cycle of vegetation phenology inferred from remote sensing is characterized by four key transition dates, which define the key phenological phases of vegetation dynamics at annual time scales. These transition dates are: (1) greenup, the date of onset of photosynthetic activity; (2) maturity, the date at which plant green leaf area is maximum; (3) senescence, the date at which photosynthetic activity and green leaf area begin to rapidly decrease; (4) dormancy, the date at which physiological activity becomes near zero. Because of the spatial, temporal, and ecological complexity of these processes, simple methods to monitor them from remote sensing have proven elusive. Here, we present a new method, which fits satellite VI data to a logistic function of time. Based on this function, the four transition dates defined above can be identified.

Field-based ecological studies have demonstrated that vegetation phenology tends to follow relatively well-defined temporal patterns. For example, in deciduous vegetation and many crops, leaf emergence tends to be followed by a period of rapid growth, followed by a relatively stable period of maximum leaf area. This pattern reflects the cumulative temperature (or more simply the number of days) from the beginning of growth, which can be easily represented using a logistic model (e.g., Ratkowski, 1983; Villegas, Aparicio, Blanco, & RoYo, 2001). The transition to senescence and dormancy follows a similar, but reverse pattern.

At regional and larger scales, variations in community composition, micro- and regional climate regimes, soils, and land management result in complex spatio-temporal variation in phenology. Further, some vegetation types exhibit multiple modes of growth and senescence within a single annual cycle. Therefore, remote sensing-based methods

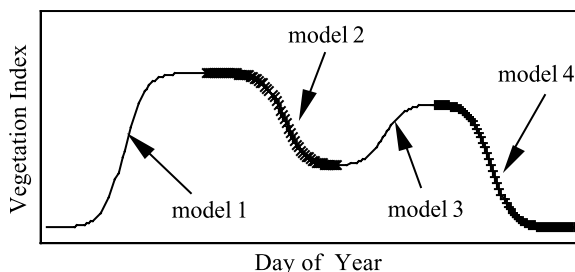


Fig. 1. An idealized trajectory of vegetation index values with multiple growth periods described using several logistic models.

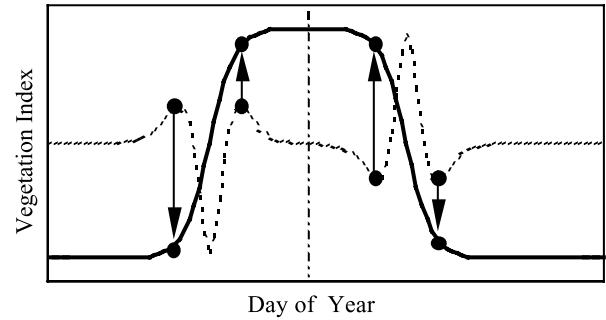


Fig. 2. A schematic showing how transition dates are calculated using minimum and maximum values in the rate of change in curvature. The solid line is an idealized time series of vegetation index data, and the dashed line is the rate of change in curvature from the VI data. The circles indicate transition dates. The extreme values located between each circle indicate the point at which the rate of change in curvature changes sign.

need to be sufficiently flexible to allow for this type of variability.

Fig. 1 shows how vegetation phenology can be represented using a series of piecewise logistic functions of time. This representation is completely general and can be used to describe the phenology of ecosystems characterized by complex behavior. Specifically, temporal variation in satellite derived VI data for a single growth or senescence cycle can be modeled using a function of the form:

$$y(t) = \frac{c}{1 + e^{a+bt}} + d \quad (1)$$

where t is time in days, $y(t)$ is the VI value at time t , a and b are fitting parameters, $c + d$ is the maximum VI value, and d is the initial background VI value. This approach is similar to the method employed by Badhwar (1980, 1984), who fit similar (exponential and logistic) smooth functions of time to approximate the variation in spectral reflectance for corn and soybean crops during growth stages. The methodology described in this paper is somewhat more general, however, because it can be used to model changes in VI data during periods of either growth or senescence.

To identify phenological transition dates, the rate of change in the curvature of the fitted logistic models is used (Fig. 2). Specifically, transition dates correspond to the times at which the rate of change in curvature in the VI data exhibits local minima or maxima. These dates indicate when the annual cycle transitions from one approximately linear stage to another. More formally, the curvature (K) for Eq. (1) at any time t can be computed using:

$$K = \frac{d\alpha}{ds} = -\frac{b^2 cz(1-z)(1+z)^3}{[(1+z)^4 + (bcz)^2]^{\frac{3}{2}}} \quad (2)$$

where $z = e^{a+bt}$, α is the angle (in radians) of the unit tangent vector at time t along a differentiable curve, and s is the unit

length of the curve. The rate of change of curvature, K' , is then:

$$K' = b^3 cz \left\{ \frac{3z(1-z)(1+z)^3 [2(1+z)^3 + b^2 c^2 z]}{[(1+z)^4 + (bcz)^2]^{\frac{5}{2}}} - \frac{(1+z)^2 (1+2z-5z^2)}{[(1+z)^4 + (bcz)^2]^{\frac{3}{2}}} \right\} \quad (3)$$

During the growth period, when vegetation transitions from a dormant state to maximum leaf area, three extreme points in a VI curve can be inferred from Eq. (3). These points correspond to the onset of leaf growth, the onset of maximum leaf area, and the inflection point between these two events (Fig. 2). Transition dates indicating the onset of senescence and dormancy can be estimated in a similar fashion.

3. MODIS data

The MODIS instrument possesses seven spectral bands that are specifically designed for land applications with spatial resolutions that range from 250 m to 1 km (Justice et al., 1997). Using daily multi-angle, cloud-free, and atmospherically corrected surface reflectances collected over 16-day periods, the MODIS bi-directional reflectance distribution function (BRDF)/Albedo algorithm generates one nadir BRDF-adjusted reflectance (NBAR) for each MODIS land band at 1-km spatial resolution (Schaaf et al., 2002). The data set used for this analysis includes 1 year

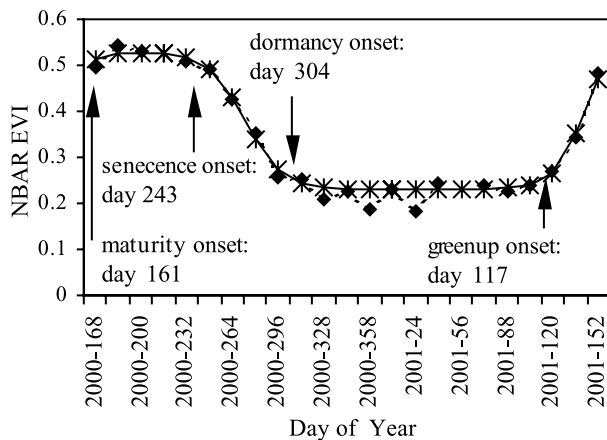


Fig. 3. A sample time series of MODIS EVI data and estimated phenological transition dates for a mixed forest pixel in New England. The dashed line with diamonds is the original EVI data and the solid line with stars is the fitted logistic models.

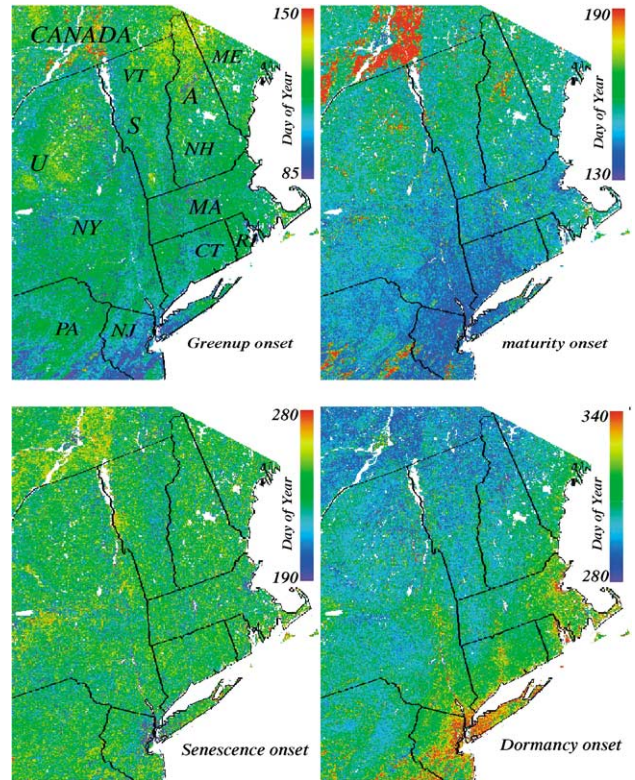


Fig. 4. Maps of phenological transition dates estimated using the method described in Section 2.

(June 9, 2000 to May 25, 2001) of NBAR time series data for a 1200- by 1200-km area centered over New England, with the exception of the 16-day periods starting on July 27, 2000 and February 2, 2001, which were not produced. To estimate the phenological models, enhanced vegetation index (EVI; Huete, Didan, Miura, & Rodriguez, 2002) values computed from NBAR data were used. Because the presence of snow can significantly affect EVI values, a normalized difference snow index (NDSI) was used to identify cases where snow or ice background was present for more than half of any given 16-day period (Hall, Riggs, & Salomonson, 1995). In cases where snow or ice was detected, the EVI value was replaced with the most recent snow-free value.

Before the NBAR EVI data could be fit to logistic functions described by Eq. (1), it was first necessary to identify periods of sustained EVI increase and decrease (i.e., growth and senescence). To do this, a moving window using five 16-day periods was applied to the annual time series. Transitions from increasing to decreasing EVI trends were then identified by a change from positive to negative slope within any given window, and vice versa. In this way, an arbitrary number of growth cycles can be identified within a given annual time series (e.g., Fig. 1). The logistic function defined by Eq. (1) was then fit to each period of EVI increase or decrease, and extreme points in the curvature rate of change were used

to identify phenological transition dates as described above.

4. Results

Fig. 3 presents representative results produced by the method described in Section 2 for a mixed forest pixel from New England. Visual inspection of this figure shows that the phenological transition dates are realistically detected. To provide a more regional perspective, Fig. 4 presents images of the northeastern United States showing the spatial variation for each of the phenological transition dates, and Fig. 5 shows the variation in greenup onset and dormancy onset as a function of latitude for different land cover types in the region. This last figure was created by computing average dates for greenup and dormancy onsets for 30-min increments of latitude within the study area, stratified by land cover classes provided by the MODIS land cover product (Friedl et al., 2002).

These figures exhibit geographically and ecologically coherent patterns that are consistent with known phenologic behavior in this region. Greenup onset occurs at the end of March or beginning of April (~85 day-of-year) in the southern zone (blue areas), with progressively later greenup in more northern zone (red and yellow areas). Within the region shown, the mean lag in greenup is 1.7 days per degree of latitude for forests and natural vegetation, and 2.2 days per degree of latitude for urban and agricultural land use. In most areas, roughly 35 days are

required from greenup onset to reach the mature phase, again with a clear trend progressing from south to north. Senescence begins between late August and September without strong spatial trend. In contrast, dormancy onset spreads southward from late October in northern areas to late November in the south. The average time lag in dormancy is about 2.4 days per degree of latitude for forests and natural vegetation, and 4.4 days for urban and agricultural land cover. Note that urban areas exhibit the earliest greenup and latest dormancy, and croplands exhibit the reverse pattern.

5. Discussion and conclusions

This communication presents a new methodology for studying vegetation phenology using remote sensing. The methodology provides a flexible means to monitor vegetation dynamics over large areas using remote sensing. Initial results using MODIS data for a region centered over New England demonstrate that the method provides realistic results that are geographically and ecologically consistent with the known behavior of vegetation in this region. In particular, the MODIS-based estimates of greenup onset, maturity onset, and dormancy onset show strong spatio-temporal patterns that also depend on land cover type.

The methodology presented in this work has several desirable properties. Since it treats each pixel individually without setting thresholds or empirical constants, the method is globally applicable. Further, it is capable of identifying phenologic behavior characterized by multiple growth and senescence periods within a single year, which is common in croplands and semiarid regions. Finally, because the method is not tied to a specific calendar period (e.g., January to December), it provides the potential to monitor vegetation phenology in near real time.

Validation is a key issue in remote sensing-based studies of phenology over large areas (Schwartz & Reed, 1999). While a variety of field programs for monitoring phenology have been initiated (e.g., Schwartz, 1999), these programs provide data that are typically species-specific and which are collected at scales that are not compatible with coarse resolution remote sensing observations. In 1-km resolution imagery, each pixel reflects the integrated response across landscapes with diverse species and phenologic behavior. While no comparisons have been made in this work between ground observations and the remote sensing-based results, this type of activity is needed to more fully understand and validate remote sensing-based observations of large-scale phenology in terrestrial vegetation.

Acknowledgements

This work was funded under NASA contract number NAS5-31369.

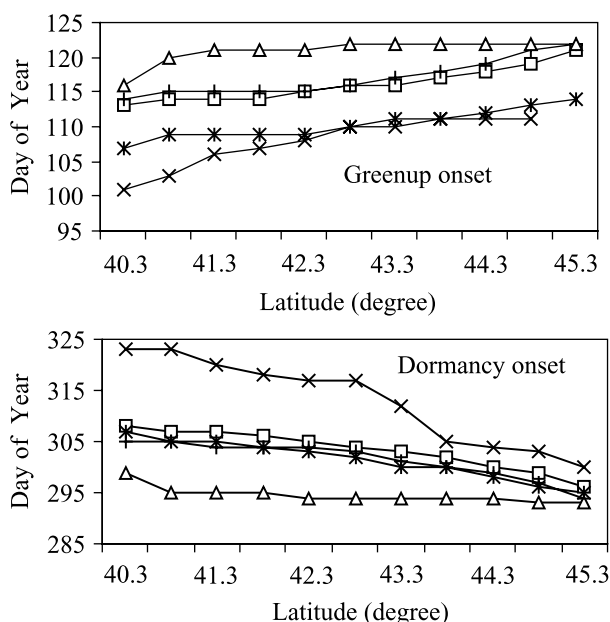


Fig. 5. Phenological transition dates averaged every 30 min of latitude for the main land cover types in the northeastern United States and southeastern Canada. □, Deciduous broad leaf forests, +, mixed forests, △, croplands, *, croplands and vegetation mosaics, ×, urban.

References

- Asrar, G., Myneni, R. B., & Kanemasu, E. T. (1989). Estimation of plant canopy attributes from spectral reflectance measurements, Chap. 7. In G. Asrar (Ed.), *Theory and applications of optical remote sensing* (pp. 252–296). New York: Wiley.
- Badhwar, G. D. (1980). Crop emergence data determination from spectral data. *Photogrammetric Engineering and Remote Sensing*, 46, 369–377.
- Badhwar, G. D. (1984). Automatic corn–soybean classification using Landsat MSS data: II. Early season crop proportion estimation. *Remote Sensing of Environment*, 14, 31–37.
- Baret, F., & Guyot, G. (1991). Potentials and limits of vegetation indices for LAI and APAR assessment. *Remote Sensing of Environment*, 35, 161–173.
- Friedl, A. F., McIver, D. K., Hodges, J. C. F., Zhang, X. Y., Muchoney, D., Strahler, A. H., Woodcock, C. E., Gopal, S., Schneider, A., Cooper, A., Baccini, A., Gao, F., & Schaaf, C. (2002). Global land cover mapping from MODIS: algorithms and early results. (Special issue) *Remote Sensing of Environment*, 83, 287–302.
- Goward, S. N., Markham, B., Dye, D. G., Dulaney, W., & Yang, A. J. (1991). Normalized difference vegetation index measurements from the Advanced Very High Resolution Radiometer. *Remote Sensing of Environment*, 35, 257–277.
- Hall, D. K., Riggs, G. A., & Salomonson, V. V. (1995). Development of methods for mapping global snow cover using moderate resolution imaging spectroradiometer data. *Remote Sensing of Environment*, 54, 127–140.
- Huete, A., Didan, K., Miura, T., & Rodriguez, E. (2002). Overview of the radiometric and biophysical performance of the MODIS vegetation indices. (Special Issue) *Remote Sensing of Environment*, 83, 195–213.
- Justice, C. O., Vermote, E., Townshend, J. R. G., Defries, R., Roy, D. P., Hall, D. K., Salomonson, V. V., Privette, J. L., Riggs, G., Strahler, A., Lucht, W., Myneni, R. B., Knyazikhin, Y., Running, S. W., Nemani, R. R., Wan, Z. M., Huete, A. R., van Leeuwen, W., Wolfe, R. E., Giglio, L., Muller, J. P., Lewis, P., & Barnsley, M. J. (1997). The moderate resolution imaging spectroradiometer (MODIS): land remote sensing for global change research. *IEEE Transactions on Geoscience and Remote Sensing*, 36, 1228–1249.
- Kaduk, J., & Heimann, M. (1996). A prognostic phenology model for global terrestrial carbon cycle models. *Climate Research*, 6, 1–19.
- Lloyd, D. (1990). A phenological classification of terrestrial vegetation cover using shortwave vegetation index imagery. *International Journal of Remote Sensing*, 11, 2269–2279.
- Moulin, S., Kergoat, L., Viovy, N., & Dedieu, G. G. (1997). Global-scale assessment of vegetation phenology using NOAA/AVHRR satellite measurements. *Journal of Climate*, 10, 1154–1170.
- Myneni, R. B., Keeling, C. D., Tucker, C. J., Asrar, G., & Nemani, R. R. (1997). Increased plant growth in the northern high latitudes from 1981–1991. *Nature*, 386, 698–702.
- Ratkowsky, D. A. (1983). *Nonlinear regression modeling—A unified practical approach* (pp. 61–91). New York: Marcel Dekker.
- Reed, B. C., Brown, J. F., VanderZee, D., Loveland, T. R., Merchant, J. W., & Ohlen, D. O. (1994). Measuring phenological variability from satellite imagery. *Journal of Vegetation Science*, 5, 703–714.
- Schaaf, C. B., Gao, F., Strahler, A. H., Lucht, W., Li, X., Tsang, T., Struwnell, N., Zhang, X. Y., Jin, Y., Muller, J. P., Lewis, P., Barnsley, M., Hobson, P., Disney, M., Roberts, G., Dunderdale, M., Doll, C., d'Entremont, R. P., Hu, B., Liang, S., & Privette, J. L. (2002). First operational BRDF, Albedo and Nadir reflectance products from MODIS. (Special Issue) *Remote Sensing of Environment*, 83, 135–148.
- Schwartz, M. D. (1999). Advancing to full bloom: planning phenological research for the 21st century. *International Journal of Biometeorology*, 42, 113–118.
- Schwartz, M. D., & Reed, B. C. (1999). Surface phenology and satellite sensor-derived onset of greenness: an initial comparison. *International Journal of Remote Sensing*, 20, 3451–3457.
- Villegas, D., Aparicio, N., Blanco, R., & RoYo, C. (2001). Biomass accumulation and main stem elongation of durum wheat grown under Mediterranean conditions. *Annals of Botany*, 88, 617–627.
- White, M. A., Thornton, P. E., & Running, S. W. (1997). A continental phenology model for monitoring vegetation responses to interannual climatic variability. *Global Biogeochemical Cycles*, 11, 217–234.